MODELING FLEXIBILITY EFFECTS IN ROBOTIC ARMS VIA THE MODIFIED 4 × 4 D-H HOMOGENEOUS TRANSFORMATIONS

A. Meghdari

Department of Mechanical Engineering
Sharif University of Technology
Tehran, Iran

M. Shahinpoor

Department of Mechanical Engineering
The University of New Mexico
Albuquerque, New Mexico, U. S. A.

Abstract **This paper presents a method for the kinematical modeling of robot manipulator arms with flexible members. Development of such techniques are important for the improvement of robotic arms precision performance and their mechanical design. The approach employs the (4×4) Denavit-Hartenberg homogeneous transformations to describe the kinematics of light weight flexible manipulator arms. The method is further applied to a two-link planar robot manipulator and a set of numerical results is generated. Comparison between the theoretical results on the two-link planar robot manipulator is quite satisfactory.**

چکیده این مقاله بیانگر روشی جهت مدلسازی سینماتیکی بازوهای مکانیکی با اعضای الاستیک میباشد. توسعه و کاربرد اینگونه روشها نقش مهمی را دربهبود دقت عمل و طراحی مکانیکی بازوهای رباتیکی دارد. این روش ماتریس‌های تبدیل همگن (۴ × ۴) دناویت-هارتنبرگ (D-H) را بمنظور توصیف سینماتیکی بازوهای الاستیک سبک‌وزن بکارمیگیرد. نهایتاً الگوی مورد بحث برای یک بازوی رباتیکی صفحه‌ای با دو درجه آزادی بکار گرفته شده است. ومقایسه محاسبات تئوریک ونتایج آزمایش روی یک ربات ساخته شده درآزمایشگاه رباتیک کاملاً رضایتبخش است.

INTRODUCTION

The robotic industry is involved in, among other things, the production of highly accurate light weight manipulators. An arm may be called upon to produce a precise tip motion. If the accuracy is measured in seconds of arc or less, then very slight deformations in the manipulator links or joints may be sufficient to produce an unacceptable motion at the end effector. Thus, it is presently becoming more important to account for small robotic tip deformations in various robotic applications. However, it is no longer possible to improve performance significantly without considering the structural deformation characteristics of the robotic elements. This is mainly because the demand for higher speed, light weight and fine precision work manipulators is increacing. Therefore, a more accurate mathematical mode that accounts for link and joint flexibility effects is one of the principal requirements for improving the robotic arm performance.

Link compliance has gained a lot of attention recently in the literature [1-3] while experimental and theoretical observations reveal that joint flexibility is the dominating source contributing to the overall robot flexibility [4-14]. In this paper, we have introduced an analytical method for modeling the kinematical behavior of robotic manipulators consisiting of both flexible links and joints. The technique presented here employs the 4×4 Denavit-Hartenberg homogeneous transformations in the presence of infinitesimal changes in the Denavit-Hartenberg joint parameters.

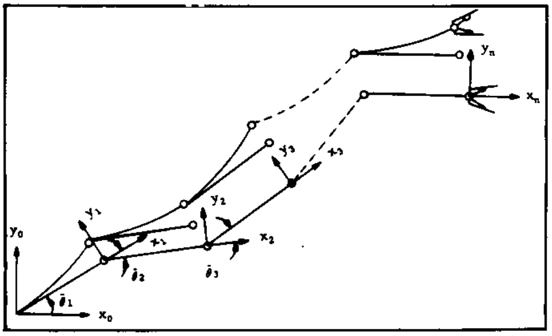

Figure 1. Flexible manipulator arm descripton

Kinematical Description of Flexible Arms

In order to describe the kinematics of the flexible manipular arm we shall consider each element of the arm with respect to its own rigid configuration as shown in Figure 1.

The Denavit - Hartenberg (D-H) Transformation ${}^{i-1}\underset{\approx}{A}_i$ describing the position and the orientation of the ith frame with respect to the (i-l)th frame in the presence of a set of infinitesimal deformations is given by:

$$ {}^{1}\underset{\approx}{A}_j = \begin{bmatrix} C\theta_i & -C\alpha_i S\theta & S\alpha_i S\theta_i & a_i C\theta_i \\ S\theta_i & C\alpha_i C\theta_i & -S\alpha_i C\theta_i & a_i S\theta_i \\ 0 & S\alpha_i & C\alpha_i & d_i \\ 0 & 0 & 0 & 1 \end{bmatrix} \qquad (1) $$

With elastic deformation taken into account it is clear that:

$$ \theta_i = \bar{\theta}_i + \delta\theta_i $$
$$ \alpha_i = \bar{\alpha}_i + \delta\alpha_i $$
$$ a_i = \bar{a}_i + \delta a_i $$
$$ d_i = d_i + \delta d_i $$

Where $\bar{\theta}_i, \bar{\alpha}_i, \bar{a}_i$ and $\bar{d}_i$ are the elastic deformation-free vectors of the joint angles link twists, link lengths, and link offsets respectively. It is worth noting that the complete composite transformation of link with respect to link i-l (joint i with respect to joint i-l) in equation (1) is found from Figure 2 and:

$$ {}^{i-1}\underset{\approx}{A}_i = \underset{\approx}{R}(z_{i-1}, \theta_i)\underset{\approx}{T}(z_{i-1}, d_i)\underset{\approx}{T}(x_i, \alpha_i)\underset{\approx}{R}(x_i, \alpha_i) $$

However, in the absence of any tip loading for a given kinematic orientation at the tip o an n-axis robotic arm, (i. e., position and orientation of the robot hand or gripper), ar inverse kinematic problem of the form:

$$ {}^{O}\underset{\approx}{\bar{T}}_i = {}^{O}\underset{\approx}{\bar{A}} \quad \underset{\approx}{\bar{A}}_2 \; {}^{2}\underset{\approx}{\bar{A}}_3 \qquad \bar{A}_i $$

Where a bar denotes no tip-loading and $\underset{\approx}{\bar{T}}$ is the 4×4 homogeneous transformation for the position and the orientation of the tip frame, can be solved. Under these conditions with no tip loading (i. e. rigid assumption):

$$ {}^{O}\underset{\approx}{\bar{T}}_i = \begin{pmatrix} \bar{n}_x & o_x & \bar{a}_x & \bar{P}_x \\ \bar{n}_y & \bar{o}_y & \bar{a}_y & \bar{P}_y \\ \bar{n}_z & \bar{o}_z & \bar{a}_z & \bar{P}_z \\ 0 & 0 & 0 & 1 \end{pmatrix} $$

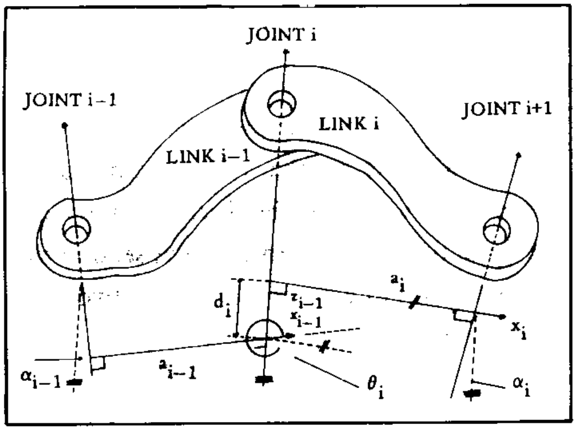

Figure 2. Danavit-Hartenberg link representation

Now let us assume that for the same given configuration a certain generalized load is applied to the tip such that the new tip frame transformation is given by:

$$\underset{\approx}{{}^0T_i} = \underset{\approx}{{}^0\bar{T}_i} + \delta\,\underset{\approx}{{}^0T_i} = \underset{\approx}{{}^0\bar{T}_i} + \begin{vmatrix} \delta n_x & \delta o_x & \delta a_x & \delta P_x \\ \delta n_y & \delta o_y & \delta a_y & \delta P_y \\ \delta n_z & \delta o_z & \delta a_z & \delta P_z \\ 0 & 0 & 0 & 0 \end{vmatrix} \qquad (9)$$

for i = 1, 2, ..., n.

Where $\delta\,\underset{\approx}{{}^0T_i}$ is the generalized elastic deformation transformation and $\delta\underset{\sim}{n}, \delta\underset{\sim}{o}, \delta\underset{\sim}{a}$, and $\delta\underset{\sim}{P}$ denote the elastic deformation vectors at the tip. Furthermore, it is clear that:

$$\underset{\approx}{{}^0T_i} = \underset{\approx}{{}^0A_1}\,\underset{\approx}{{}^1A_2}\,\underset{\approx}{{}^2A_3} \cdots \underset{\approx}{{}^{i-1}A_i} \qquad (10)$$

Where, generally speaking:

$$\underset{\approx}{{}^{i-1}A_i} = \underset{\approx}{{}^{i-1}\bar{A}_i} + \delta\,\underset{\approx}{{}^{i-1}A_i} \qquad (1$$

Where $\delta\,\underset{\approx}{{}^{i-1}A_i}$ denotes a 4×4 homogeneous transformation indicating the generalized elastic deformation of the ith frame with respect to the (i-l)th frame. Note that under these circumstances:

$$\delta\,\underset{\approx}{{}^{i-1}A_i} = f(\bar{\theta}_i, \bar{\alpha}_i; \bar{a}_i, \bar{d}_i, \delta\theta_i, \delta\alpha_i, \delta a_i, \delta d_i) \qquad (12)$$

For infinitesimal elastic deformations one may neglect the higher order terms in applying equations (1) and (11) so that $\delta\,\underset{\approx}{{}^{i-1}A_i}$ is the result:

$$\delta^{1}\,\underset{\approx}{A_i} = \begin{vmatrix} -\delta\theta_i S\bar{\theta}_i & \delta\alpha_i S\bar{\alpha}_i S\bar{\theta}_i - \delta\theta_i C\bar{\alpha}_i C\bar{\theta}_i & \delta\theta_i S\bar{\alpha}_i C\bar{\theta}_i + \delta\alpha_i C\bar{\alpha}_i S\bar{\theta}_i & \delta a_i C\bar{\theta} - \delta\theta_i \bar{a}_i S\bar{\theta}_i \\ \delta\theta_i C\bar{\theta}_i & -\delta\theta_i S\bar{\theta}_i C\bar{\alpha}_i - \delta\alpha_i S\bar{\alpha}_i C\bar{\theta}_i & \delta\theta_i S\bar{\theta}_i S\bar{\alpha}_i - \delta\alpha_i C\bar{\alpha}_i C\bar{\theta}_i & \delta a_i S\bar{\theta}_i + \delta\theta_i \bar{a}_i C\bar{\theta}_i \\ 0 & \delta\alpha_i C\bar{\alpha}_i & \delta\alpha_i S\bar{\alpha}_i & \delta d_i \\ 0 & 0 & 0 & 0 \end{vmatrix} \qquad (13)$$

Furthermore, the generalized elastic deformation 4×4 homogeneous transformation $\delta\,\underset{\approx}{{}^0T_i}$ is now related to $\delta\,\underset{\approx}{{}^{i-1}A_i}$ through an expanded and linearized version of equations (9), (10), and (11) such that:

$$\begin{aligned} \delta\,\underset{\approx}{{}^0T_i} = {} & \delta\,\underset{\approx}{{}^0A_1}\,\underset{\approx}{{}^1\bar{A}_2}\,\underset{\approx}{{}^2\bar{A}_3} \cdots {}^{i-1}\bar{A}_i + \\ & \underset{\approx}{{}^0\bar{A}_1}\,\delta\,\underset{\approx}{{}^1\bar{A}_2}\,\underset{\approx}{{}^2\bar{A}_3} \cdots \underset{\approx}{{}^{i-1}\bar{A}_i} + \\ & \underset{\approx}{{}^0\bar{A}_1}\,\underset{\approx}{{}^1\bar{A}_2}\,\delta\,\underset{\approx}{{}^2A_3} \cdots \underset{\approx}{{}^{i-1}\bar{A}_i} + \\ & + \underset{\approx}{{}^0\bar{A}_1}\,\underset{\approx}{{}^1\bar{A}_2}\,\underset{\approx}{{}^2\bar{A}_3} \cdots \delta\,\underset{\approx}{{}^{i-2}A_{i-1}}\,\underset{\approx}{{}^{i-1}\bar{A}_i} \\ & + \underset{\approx}{{}^0\bar{A}_1}\,\underset{\approx}{{}^1\bar{A}_2}\,\underset{\approx}{{}^2\bar{A}_3} \cdots \underset{\approx}{{}^{i-2}\bar{A}_{i-1}}\,\delta\,\underset{\approx}{{}^{i-1}A_i} \end{aligned} \qquad (14)$$

for i =1, 2, ..., n

From equations (9), (13), and (14) the tip deformation vectors $\delta \underset{\sim}{n}, \delta \underset{\sim}{o}, \delta \underset{\sim}{a}$ and $\delta \underset{\sim}{P}$ can be clearly related to the joint deformation quantities $\delta\theta_i, \delta\alpha_i, \delta a_i$ and δd_i such that:

$$\delta \underset{\sim}{n} = \underset{\sim}{f_1} (\bar{\theta}_i, \bar{\alpha}_i, \bar{a}_i, \bar{d}_i, \delta\theta_i, \delta\alpha_i, \delta a_i, \delta di) \quad (15)$$

$$\delta \underset{\sim}{o} = \underset{\sim}{f_2} (\bar{\theta}_i, \bar{\alpha}_i, \bar{a}_i, \bar{d}_i, \delta\theta_i, \delta\alpha_i, \delta a_i, \delta d_i) \quad (16)$$

$$\delta \underset{\sim}{a} = \underset{\sim}{f_3} (\bar{\theta}_i, \bar{\alpha}_i, \bar{a}_i, \bar{d}_i, \delta\theta_i, \delta\alpha_i, \delta a_i, \delta d_i) \quad (17)$$

$$\delta \underset{\sim}{P} = \underset{\sim}{f_4} (\bar{\theta}_i, \bar{\alpha}_i, \bar{a}_i, \bar{d}_i, \delta\theta_i, \delta\alpha_i, \delta a_i, \delta di) \quad (18)$$

Now one can directly relate the joint elastic deformation variables $\delta\theta_i, \delta\alpha_i, \delta\alpha_i$, and δd_i to local structural and materials properties as well as the local generalized force vector $^A\underset{\sim}{F}$ such that:

$$^A\underset{\sim}{F} = \begin{bmatrix} ^Af_x \\ ^Af_y \\ ^Af_z \\ ^A\tau_x \\ ^A\tau_y \\ ^A\tau_z \end{bmatrix} = {^A\underset{\approx}{J_f}}^T \underset{\sim}{F} = {^A\underset{\approx}{J_f}}^T \begin{bmatrix} f_x \\ f_y \\ f_z \\ \tau_x \\ \tau_y \\ \tau_z \end{bmatrix} \quad (19)$$

Where A is the local frame $^{i-1}\underset{\approx}{A}_i$ with respect to which the elastic deformation variables are measured, $^A\underset{\sim}{F}$ is generalized local force applied at the joint to which frame $^{i-1}\underset{\approx}{A}_i$ is attached, $^A\underset{\approx}{J_f}^T$ is the transpose of the flexible Jacobian of force transformations between the tip frame $^0\underset{\approx}{T}_i$ and the A frame. $\underset{\sim}{F}$ is the generalized force vector applied at the robotic tip frame, where $\underset{\sim}{f}$ and τ are the force and couple vectors, respectively. In the next section the above technique is applied to a two link planar robot manipulator.

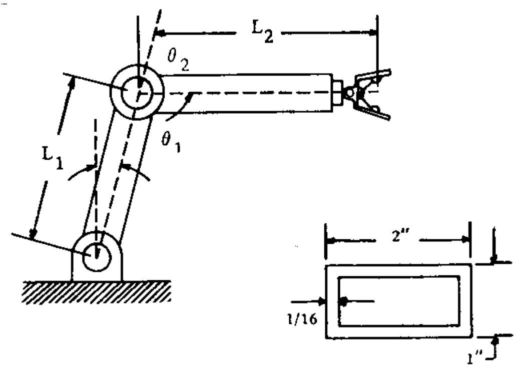

Figure 3. A simple two-link flexible planar arm

Application of the Generalized Technique to a Flexible Two-link Planar Arm

In order to observe the various steps involved in the implementation of the generalized technique, let us consider a special case of a flexible two-link planar arm with revolute joints as shown in Figure 3. Let us further assign the appropriate link coordinate frames to the mechanism and establish the table of joint parameters represented by Table 1.

It should be noted that in our analysis we have considered the robotic link elements to

Table 1. Table of Joint Parameters for the Flexible Arm

Joint	$\theta_i = \bar{\theta}_i + \delta\theta_i$	$\alpha_i = \bar{\alpha}_i + \delta\alpha_i$	$a_i = \bar{a}_i + \delta a_i$	$d_i = \bar{d}_i + \delta d_i$	$\sin\alpha_i$	$\cos\alpha_i$
1	$\theta_1 + \delta\theta_1$	0	$\ell_1 + \delta\ell_1$	0	0	1
2	$\theta_2 + \delta\theta_2$	0	$\ell_2 + \delta\ell_2$	0	0	1

be straight bars of uniform cross section capable of resisting axial forces as well as bending moments. We further assume that the robotic links are inextensible. Within this assumption the changes in the link lengths reduce to an almost insignificant amount. Therefore $\delta \ell_1 = \delta \ell_2 \approx 0$. Knowing these facts, one can easily find the corresponding transformation matrices ${}^0\underset{\approx}{A}_1$, and ${}^1\underset{\approx}{A}_2$ representing the position and orientation of the first link with respect to the base frame, and second link relative to the first link, respectively.

$$ {}^0\underset{\approx}{A}_1 = {}^0\underset{\approx}{\bar{A}}_1 + \delta\, {}^0\underset{\approx}{A}_1 = \begin{vmatrix} C(\bar{\theta}_1+\delta\theta_1) & -S(\bar{\theta}_1+\delta\theta_1 & 0 & \ell_1 C(\bar{\theta}_1+\delta\theta_1) \\ S(\bar{\theta}_1+\delta\theta_1) & C(\bar{\theta}_1+\delta\theta_1) & 0 & \ell_1 S(\bar{\theta}_1+\delta\theta_1) \\ 0 & 0 & & 0 \\ 0 & 0 & 0 & \end{vmatrix} \quad (20) $$

and

$$ \underset{\approx}{A}_2 = {}^1\underset{\approx}{\bar{A}}_2 + \delta\, {}^1\underset{\approx}{A}_2 = \begin{vmatrix} C(\bar{\theta}_2+\delta\theta_2) & -S(\bar{\theta}_2+\delta\theta_2) & 0 & \ell_2 C(\bar{\theta}_2+\delta\theta_2) \\ S(\bar{\theta}_2+\delta\theta_2) & C(\bar{\theta}_2+\delta\theta_2) & 0 & \ell_2 S(\bar{\theta}_2+\delta\theta_2) \\ 0 & 0 & 1 & 0 \\ 0 & 0 & 0 & 1 \end{vmatrix} \quad (21) $$

Where the $\delta\theta$'s actually represent the infinitesimal rotations of the servo motor plus the slope of robotic link deflection at the joint as shown in Figure 4. In other words:

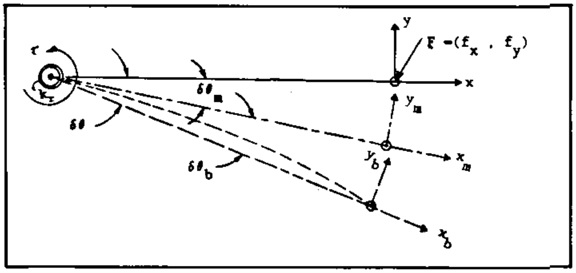

Figure 4. A robotic link element with flexible members

$$ \delta\theta_1 = \delta\theta_{1_b} + \delta\theta_m \qquad (22a) $$

$$ \delta\theta_2 = \delta\theta_{2_b} + \delta\theta_{2_m} \qquad (22b) $$

where:

$\delta\theta_{1_b}, \delta\theta_{2_b}$: are the slopes of the robotic links deflections.

$\delta\theta_{1m}, \delta\theta_{2_m}$: are the infinitesimal rotations of the servo motors.

Utilizing equations (9-13) the position and orientation of the end effector with respect to the base frame in the presence of deformations are obtained. Thus:

$$ {}^0\underset{\approx}{T}_2 = {}^0\underset{\approx}{A}_1 {}^1\underset{\approx}{A}_2 = {}^0\underset{\approx}{\bar{T}}_2 + \delta\, {}^0\underset{\approx}{T}_2 = $$

$$ \begin{vmatrix} C_{12} & -S_{12} & 0 & \ell_2 C_{12} + \ell_1 C_1 \\ S_{12} & C_{12} & 0 & \ell_2 S_{12} + \ell_1 S_1 \\ 0 & 0 & 1 & 0 \\ 0 & 0 & 0 & 1 \end{vmatrix} + \delta\, {}^0\underset{\approx}{T}_2 $$

Where $C_{12} = \cos(\bar{\theta}_1 + \bar{\theta}_2)$, $S_{12} = \sin(\bar{\theta}_1 + \bar{\theta}_2)$, $C_1 = \cos\bar{\theta}_1$, $S_1 = \sin\bar{\theta}_1$, and

$$ \delta\, {}^0\underset{\approx}{T}_2 = \delta\, {}^0\underset{\approx}{A}_1 {}^1\underset{\approx}{\bar{A}}_2 + {}^0\underset{\approx}{\bar{A}}_1 \delta\, {}^1\underset{\approx}{A}_2 $$

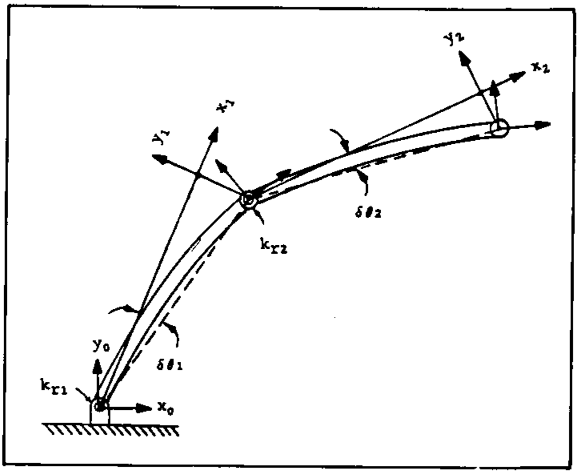

Figure 5. A simple arm with flexible links and joints.

$$\delta\,{}^0A_1 = \begin{bmatrix} -\delta\theta_1 S_1 & -\delta\theta_1 C_1 & 0 & -\delta\theta_1 \ell_1 S_1 \\ \delta\theta_1 C_1 & -\delta\theta_1 S_1 & 0 & \delta\theta_1 \ell_1 C_1 \\ 0 & 0 & 0 & 0 \\ 0 & 0 & 0 & 0 \end{bmatrix} \qquad (25)$$

$$\delta\,{}^1\underset{\approx}{A_2} = \begin{bmatrix} -\delta\theta_2 S_2 & -\delta\theta_2 C_2 & 0 & -\delta\theta_2 \ell_2 S_2 \\ \delta\theta_2 C_2 & -\delta\theta_2 S_2 & 0 & \delta\theta_2 \ell_2 C_2 \\ 0 & 0 & 0 & 0 \\ 0 & 0 & 0 & 0 \end{bmatrix} \qquad (26)$$

Substituting equations (25) and (26) into equation (24) will result in:

$$\delta\,{}^0\underset{\approx}{T_2} = \begin{bmatrix} -(\delta\theta_1+\delta\theta_2)S_{12} & -(\delta\theta_1+\delta\theta_2)C_{12} & 0 & -(\delta\theta_1+\delta\theta_2)\ell_2 S_{12} - \delta\theta_1 \ell_1 S_1 \\ (\delta\theta_1+\delta\theta_2)C_{12} & (\delta\theta_1+\delta\theta_2)S_{12} & 0 & (\delta\theta_1+\delta\theta_2)\ell_2 C_{12} + \delta\theta_1 \ell_1 C_1 \\ 0 & 0 & 0 & 0 \\ 0 & 0 & 0 & 0 \end{bmatrix} \qquad (27)$$

where $C_{12} = \mathrm{Cos}(\bar\theta_1+\bar\theta_2)$, and $S_{12} = \mathrm{Sin}(\bar\theta_1+\bar\theta_2)$. From expressions (23) and (27) it is obvious that, to perform the direct kinematic of the arm under loading conditions, one has to compute the infinitesimal rotations $\delta\theta_1$ and $\delta\theta_2$. To evaluate these unknowns, we consider a force vector $\underset{\sim}{F}$ applied at the tip of the arm. Then by means of the flexible manipulator Jacabian $(\underset{\approx}{J_f})$ we can find the corresponding joint forces and torques as a function of configuration and the applied tip force. For the two link arm under consideration one may readily show that:

$$\begin{bmatrix} \tau_1 \\ \tau_2 \end{bmatrix} = \begin{bmatrix} \ell_1 S(\bar\theta_2+\delta\theta_2) & \ell_2+\ell_1 C(\bar\theta_2+\delta\theta_2) \\ 0 & \ell_2 \end{bmatrix} \begin{bmatrix} f_x \\ f_y \end{bmatrix} \qquad (28)$$

where:

$$\underset{\approx}{J_f}^T = \begin{bmatrix} \ell_1 S(\bar{\theta}_2+\delta\theta_2) & 0 \\ \ell_2+\ell_1 C(\bar{\theta}_2+\delta\theta_2) & \ell_2 \end{bmatrix} \quad (29)$$

is the transpose of the corresponding flexible Jacabian. Since $\delta\theta$'s are very small ($\mathrm{Sin}(\delta\theta) \simeq \delta\theta$ and $\mathrm{Cos}(\delta\theta) \simeq 1$), therefore equation (29) becomes:

$$J_f^T = \begin{bmatrix} \ell_1(S_2+\delta\theta_2 C_2) & 0 \\ \ell_2+\ell_1(C_2-\delta\theta_2 S_2) & \ell_2 \end{bmatrix} \quad (30)$$

where:

$\delta\theta_2 = \delta\theta_{2_b} + \delta\theta_{2_m}$. Since the effects of axial deformations are neglected in the analysis, no matter how the tip force vector $\underset{\sim}{F}$ is applied, only its fy component is the dominant force in contributing to the slope of the deflection curve for the second link and joint. Hence from basic mechanics we have:

$$\delta\theta_{2_b} = \frac{f_y \ell_2^2}{3E_2 I_2} \quad (31)$$

and

$$\delta\theta_{2_m} = \frac{\tau^2}{k_{r_2}} \quad (32)$$

where Kr_2 is the equivalent rotational stiffness coefficient of the second joint which can be measured since it purely depends on the joint design, armature current, and the type of motor used. Substituting equations (31) and (32) into equation (30) and then into equation (28) will result in:

$$\tau_1 = \ell_1 [S_2 + [\frac{\ell_2}{k_{r2}} + \frac{\ell_2^2}{3E_2 I_2}] C_2 f_y] f_x + [\ell_2 + \ell_1 [C_2 - [\frac{\ell_2}{k_{r2}} + \frac{\ell_2^2}{3E_2 I_2} S_2 f_y]] f_y \quad (33)$$

$$\tau_2 = \ell_2 f_y \quad (34)$$

By knowing τ_1 and τ_2 it is now possible to evaluate $\delta\theta_1$ which is:

$$\delta\theta_1 = \delta\theta_{1_b} + \delta\theta_{1_m} \quad (22a)$$

where:

$$\delta\theta_{1_b} = \frac{f_{y1}\ell_1^2}{3E_1 I_1}, \text{ and} \quad (35)$$

$$\delta\theta_{1_m} = \frac{\tau_1}{k_{r_1}} \quad (36)$$

where Kr_1 is the equivalent rotational stiffness coefficient of the first joint and:

$$f_{y_1} = f_x S(\bar{\theta}_2+\delta\theta_2) + f_y C(\bar{\theta}_2+\delta\theta_2) \quad (37)$$

or

$$f_{y_1} = f_x [S_2+\delta\theta_2 C_2] + f_y [C_2-\delta\theta_2 S_2] \quad (38)$$

Once $\delta\theta_1$ and $\delta\theta_2$ are evaluated for a given tip force $\underset{\sim}{F}$, then by substituting the results into equations (23) and (27) the position and orientation of a statically loaded manipulator under infinitesimal deformation are computed.

$$ {}^{0}\underset{\approx}{T}_2 = {}^{0}\bar{\underset{\approx}{T}}_2 + \delta\,{}^{0}\underset{\approx}{T}_2 \qquad (39)$$

Knowing the actual position, one can readily compensate for the positional error $\delta\,{}^{0}\underset{\approx}{T}_2$ to achieve the desired position and orientation of the end effector ${}^{O}\bar{\underset{\approx}{T}}_2$.

The inverse kinematics problem of this flexible arm may be stated as:

"Given the actual position and orientation of the robot arm gripper under a tip loading vector $\underset{\sim}{F}$, ${}^{0}\underset{\approx}{T}_2$, what are the corresponding values of the joint angles θ_1 and θ_2". Therefore, consider ${}^{0}\underset{\approx}{T}_2$ as being the transformation representing the actual position and orientation of the end effector

$$ {}^{0}\underset{\approx}{T}_2 = \begin{vmatrix} n_x & o_x & a_x & P_x \\ n_y & o_y & a_y & P_y \\ n_z & o_z & a_z & P_z \\ 0 & 0 & 0 & \end{vmatrix} \qquad (40)$$

and a force vector $\underset{\sim}{F} = [f_x, f_y]$ applied at the tip. To solve for θ_1 and θ_2, an inverse kinematic solution of the form

$$\theta_2 = \bar{\theta}_2 + \delta\theta_2 = \text{atan2}(S\theta_2/C\theta_2) \qquad (41)$$

where:

$$C\theta_2 = \frac{P_x^2 + P_y^2 - \ell_1^2 - \ell_2^2}{2\ell_1\ell_2}$$

$$\text{and } S\theta_2 = \pm\sqrt{1 - [C\theta_2]^2}$$

and,

$$\theta_1 = \bar{\theta}_1 + \delta\theta_1 = \text{atan2}\,(P_x/P_y) - \text{atan2}\,[\ell_2 S\theta_2/(\ell_1 + \ell_2 C\theta_2)] \qquad (42)$$

may be used. Once θ_1 and θ_2 are computed in order to evaluate $\delta\theta_1$ and $\delta\theta_2$, one may use equations (28), (31), (32), (37), (35), (36), and (22) accordingly.

NUMERICAL RESULTS AND CONCLUSIONS

Let us consider the arm shown in Figure 5 with the following specifications, and a vertical tip loading of $\underset{\sim}{F} = [O, -8]$.

$\ell_1 = \ell_2 = 22$ (inches)

$E_1 = E_2 = 10 \times 10^6$

$I_1 = I_2 = 0.0619914$

$A_1 = A_2 = 0.3594$

$k_{r_1} \simeq 35000$ (1b−in)

$k_{r_2} \simeq 30000$ (1b−in)

$\bar{\theta}_1 = 45°$

$\bar{\theta}_2 = -45°$

Therefore, for this configuration by utilizing equations (33) and (34) we have;

$\tau_1 = -229.462$ (1b−in)

and

$\tau_2 = -176.0$ (1b−in)

and further from equations (22), (31), (32), (35), (36), and (38) we have:

$\delta\theta_2 = -0.00208201 - 0.0058667 = -0.00794868$ (radians)

and,

$f_{y_1} = 5.61189$ (1bs.)

$\delta\theta_1 = -0.0014605 \quad 0.008556 = -0.0100165$ (radians)

Now from equations (23) and (27), we have:

$$
{}^{0}T_2 = {}^{0}\bar{\underset{\approx}{T}}_2 + \delta\, {}^{0}\underset{\approx}{T}_2 =
\underbrace{\underset{\text{Desired position}}{\begin{bmatrix} 1 & 0 & 0 & 37.5564 \\ 0 & 1 & 0 & 15.5563 \\ 0 & 0 & 1 & 0 \\ 0 & 0 & 0 & 1 \end{bmatrix}} + \begin{bmatrix} 0 & 0.017977 & 0 & 0.1558 \\ -0.017977 & 0 & 0 & -0.5511 \\ 0 & 0 & 0 & 0 \\ 0 & 0 & 0 & 0 \end{bmatrix}}_{\text{Actual position}}
$$

Figure 6 displays the robotic arm trajectory under gravity loading of 8 lbs. applied at the tip. Configuration of the arm was chosen so that the first link was kept at a 45°joint angle where as the second link was let to vary its position and orientation from +45°to -45°joint angle with increments of 5°. The desired trajectory is represented by the positions and orientations at which the robot gripper must be under loading (with no deformations) whereas the actual trajectory is the actual positions and orientations of the gripper due to the joint and link deformations.

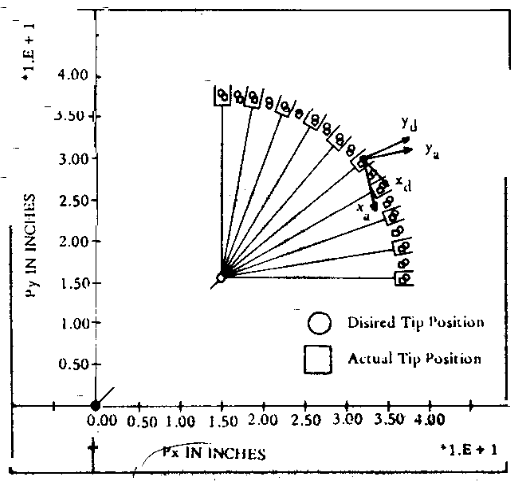

Figure 6. The robotic arm tip trajectory under gravity loading of 8 lbs.

Comparison between the theoretical and experimental results on a two-link planar robot manipulator built and tested in our robotic instructional and research laboratory illustrated in Figure 7 is quite satisfactory.

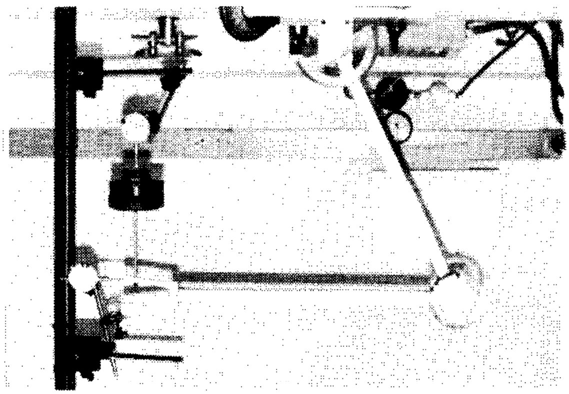

Figure 7. Experimental set up.

ACKNOWLEDMENT

The authors wish to thank Mrs. Shari L. Meghdari for the preparation of the typed manuscript.

REFERENCES

1. G. M. Dick. In: M. Jamshidi, J Y. S. Luh and M. Shahinpoor (eds), "Proceedings of the International Symposium on Robot Manipulators." p. 137 Albuguerue, N. M.(1986).
2. Ahmad and G. R. Widmann,'Active Joint Stiffness

Compensation in Robot Arms." Presented at the Conference on Applied Motion Control, Minneapolis, MN. (1985).
3. H. B. Kuntze and A. H. K. Jacubasch, *IEEE J. of Robotics and Automation* RA-1, 71. (1985).
4. A. Megdari and M. Shahinpoor, *Internat. J. of Robotics Automation,* IASTED, 2. (1987).
5. E. F. Rivin. Proceeding of the 1985 American Control Conference, p. 381, Boston, MA (1985).
6. M. Shahinpoor and A. Meghdari, *Robotica Internat.* J. 4, 237 (1986).
7. W. J. Books. *J. Dynamic Systems Measurement and Control.* 101, 187 (1979).
8. F. A. Kelly and R. L. Huston , "Modeling Flexibility Effects in Robot Arms." Proceedings of 1981 Joint Automatic Control Conf. 1 (1981).
9. G. R. Wismann and S. Ahman, In: M. Jamshidi, J. Y. S. Luh and M. Shahinpoor (eds) "Proceedings of the International Symposium on Robot Manipulators, P. 145. Albuguergue, NM (1986).
10. E. I. Rivin, Analysis of Structural Compliane for Robot Manipulators." In: S. N. Dwiveed (ed) "Proceedings of an International Conference." Charlotte NC (1984).
11. A. Meghdari, Ph. D. Dissertation, University of New Mexic, Albuguergue, NM (1987).
12. A. Meghdari and M. Shahinpoor. *Robotica Internal. J.* 6, 203 (1988).
13. A. Meghdari, Robotica Internat. J. in press (1990).
14. A. Meghdari, In: "Proceeding of the IASTED Conference on Control and Modeling, P. 484. Tehran, Iran (1990).